

# Rapid pacing of embryoid bodies impairs mitochondrial ATP synthesis by a calcium-dependent mechanism—A model of in vitro differentiated cardiomyocytes to study molecular effects of tachycardia

Lorenz Schild<sup>a</sup>, Alicja Bukowska<sup>b</sup>, Andreas Gardemann<sup>a</sup>, Pamela Polczyk<sup>b,f</sup>, Gerburg Keilhoff<sup>c</sup>, Michael Täger<sup>d</sup>, Samuel C. Dudley<sup>e</sup>, Helmut U. Klein<sup>f</sup>, Andreas Goette<sup>f,\*</sup>, Uwe Lendeckel<sup>b,1</sup>

<sup>a</sup> Institute of Clinical Chemistry, Department of Pathobiochemistry, Otto-von-Guericke University Magdeburg, Germany

<sup>b</sup> Institute of Experimental Internal Medicine, Otto-von-Guericke University Magdeburg, Germany

<sup>c</sup> Institute of Medical Neurobiology, Otto-von-Guericke University Magdeburg, Germany

<sup>d</sup> IMTM Magdeburg, Germany

<sup>e</sup> Division of Cardiology, Emory University School of Medicine, Atlanta, GA 30322, USA

<sup>f</sup> Division of Cardiology, University Hospital Magdeburg, Leipzigerstr. 44 39120 Magdeburg, Germany

Received 22 November 2005; received in revised form 17 March 2006; accepted 20 March 2006

Available online 19 April 2006

## Abstract

Tachycardia may cause substantial molecular and ultrastructural alterations in cardiac tissue. The underlying pathophysiology has not been fully explored. The purpose of this study was (I) to validate a three-dimensional in vitro pacing model, (II) to examine the effect of rapid pacing on mitochondrial function in intact cells, and (III) to evaluate the involvement of L-type-channel-mediated calcium influx in alterations of mitochondria in cardiomyocytes during rapid pacing. In vitro differentiated cardiomyocytes from P19 cells that formed embryoid bodies were paced for 24 h with 0.6 and 2.0 Hz. Pacing at 2.0 Hz increased mRNA expression and phosphorylation of ERK1/2 and caused cellular hypertrophy, indicated by increased protein/DNA ratio, and oxidative stress measured as loss of cellular thiols. Rapid pacing additionally provoked structural alterations of mitochondria. All these changes are known to occur in vivo during atrial fibrillation. The structural alterations of mitochondria were accompanied by limitation of ATP production as evidenced by decreased endogenous respiration in combination with decreased ATP levels in intact cells. Inhibition of calcium inward current with verapamil protected against hypertrophic response and oxidative stress. Verapamil ameliorated morphological changes and dysfunction of mitochondria. In conclusion, rapid pacing-dependent changes in calcium inward current via L-type channels mediate both oxidative stress and mitochondrial dysfunction. The in vitro pacing model presented here reflects changes occurring during tachycardia and, thus, allows functional analyses of the signaling pathways involved.

© 2006 Elsevier B.V. All rights reserved.

**Keywords:** Arrhythmia; Hypertrophy; Myocyte; Oxidative stress; Pacing; Mitochondria

## 1. Introduction

It has been shown in animal models of chronic cardiac tachycardia that rapid irregular stimulation of the atrium causes detrimental effects in this tissue [1–5]. Electrophysiological changes such as reduction of the refractory period, which results

in electrical remodeling, have been reported [1–3]. There is a body of evidence demonstrating that  $\text{Ca}^{2+}$  influx into the cardiomyocytes mediates this response to chronic cardiac tachyarrhythmia [2,3]. Studies using atrial tissue have shown that a tachycardia-induced  $\text{Ca}^{2+}$  overload of cardiomyocytes causes substantial shortening of the atrial action potential, impairment of contractility, cellular hypertrophy, and induces ultrastructural alterations such as morphologically altered mitochondria and disrupted endoplasmic reticulum [1–7]. Moreover, a recent study has provided the first evidence of the

\* Corresponding author. Tel.: +49 391 6713203; fax: +49 391 673202.

E-mail address: [andreas.goette@medizin.uni-magdeburg.de](mailto:andreas.goette@medizin.uni-magdeburg.de) (A. Goette).

<sup>1</sup> Both authors contributed equally to this study.

involvement of oxidative stress in cardiac tachycardia [8,9]. Carnes et al. have demonstrated an increase in the concentration of reactive oxygen species associated with increased amounts of oxidatively modified proteins during electrical remodeling [8].

Although tachycardia-induced alterations in the mitochondrial morphology of cardiomyocytes have been demonstrated, limited data are available regarding the effect of tachycardia on mitochondrial function. It has been shown in *in vivo* studies and *in vitro* that atrial fibrillation is associated with a higher demand of energy of cardiomyocytes, resulting in transiently decreased concentrations of high-energy phosphates and mitochondrial NADH [10,11]. There are controversial reports concerning the effect of tachyarrhythmia, such as atrial fibrillation, on the activity of mitochondrial enzymes. Using a canine model, decreased activities of mitochondrial complexes III and V have been reported during rapid pacing [12], whereas no changes were found in the activities of complexes IV and V in goats subjected to atrial fibrillation [11]. Reduced ATP levels have been described in human right atrial tissue samples, but it remains unclear whether these are due to mitochondrial dysfunction or increased ATP consumption in the cardiomyocytes [13]. Here, we address this question by analyzing the effect of tachycardia on mitochondrial function and adenine nucleotide concentration in intact cardiomyocytes.

Reliable information about the effect of tachycardia on mitochondrial function is of particular importance since mitochondrial dysfunction can result in the induction of apoptosis or necrosis. The purpose of the present study was to characterize mitochondrial function after cardiac tachycardia, and to elucidate the role of  $\text{Ca}^{2+}$  influx via L-type channels in the induction of mitochondrial alterations. Therefore, we analyzed mitochondrial respiration and the concentration of cellular adenine nucleotides in response to rapid pacing.

In order to reduce the number of animal experiments, we developed a tachycardia model using *in vitro* differentiated cardiomyocytes. These cells form three-dimensional embryoid bodies (EBs) that consist of a heterogeneous mixture of cells including pace-maker, contractile (and excitable to various extents) and non-contractile cells. In contrast to isolated pure myocyte cultures, EBs reflect the myocardial tissue architecture reasonably well. Rapid pacing of these electrically well-coupled cardiomyocytes derived from P19 cells [14–18] causes stimulation of Erk-2 expression, mitochondrial swelling, and cellular hypertrophy, as previously shown in *in vivo* studies [19,20]. In this study, we found that rapid pacing of EBs caused a verapamil-sensitive decrease in respiration and cellular ATP.

## 2. Materials and methods

### 2.1. Differentiation of cardiomyocytes

Mouse P19 cell lines were used throughout the study. Because of the lack of electrical coupling and synchronicity in cultures of isolated cardiomyocytes, we used an *in vitro* differentiation model leading to a three-dimensional embryoid body, which consists of electrically coupled cells with synchronized spontaneous contractions. In contrast to embryonic stem cells requiring feeder cells for culture, P19 cells are relatively robust and do not depend on the presence of additional cells in culture [14–18]. Undifferentiated (pluripotent) P19 cells (ATCC CRL-1825)

were maintained and passaged in high-glucose DMEM (Gibco BRL) supplemented with 15% FBS, 200 mmol/l L-glutamine,  $5 \times 10^{-5}$  mol/l 2-mercaptoethanol, 10 mmol/l non-essential amino acids, and 5000 U/ml penicillin/streptomycin. P19 cells were expanded on 0.1% gelatin-coated petri dishes in monolayers to 80% confluence before they were split. Differentiation was initiated by suspending 400–800 P19 cells in 20  $\mu\text{l}$  of medium, supplemented with 15% FBS and 1% DMSO, as hanging drops for 2 days. The resulting embryoid bodies (EBs) were cultured for 5 days in suspension. Seven-day-old EBs were then plated onto petri dishes. *In vitro* differentiation of P19 cells into cardiomyocytes was demonstrated at the molecular level by the expression of GATA-4,  $\alpha$ -myosin heavy chain (MHC) and  $\beta$ -MHC (not shown).

### 2.2. *In vitro* pacing model

To stimulate the differentiated cardiomyocytes of EBs, a pair of custom-built carbon electrodes ( $12.5 \times 6 \times 32$  mm) was submerged at opposite sides of a petri dish in medium. The distance between the electrodes was about 8 cm. Copper wires, which were electrically isolated with silicon rubber, were inserted into holes drilled into the carbon electrodes and connected to a stimulation unit (GRASS Stimulator). A biphasic square wave impulse of 150 V total amplitude and 5 ms duration was used for stimulation. The biphasic impulse (encompassing a positive and negative deflection) was used to minimize electrolysis at the electrodes. All EBs were located in the center of the petri dish (minimum distance to each electrode: 3 cm). Synchronous contractions of the EBs at the applied pacing frequency was verified by microscopy. Three hertz was the fastest frequency rate that resulted in 1:1 capture of the EB. Pacing of EBs was performed in the cell culture incubator for up to 24 h at 37 °C, at pacing frequencies of 0.6 Hz (bradycardia) and 2.0 Hz (tachycardia). The spontaneous frequency of EB contractions was approximately 0.5 Hz. The culture medium was changed daily over the course of the experiments. To analyze the effect of  $\text{Ca}^{2+}$  influx into the cardiomyocytes on the impairment of the cells due to pacing, 0.1  $\mu\text{M}$  verapamil was added to the medium throughout the electrical treatment.

### 2.3. Determination of the protein/DNA ratio

DNA and protein contents were determined simultaneously in each sample of P19 EBs. DNA was extracted by using the InViSorb Genomic DNA Kit I (InViTek, Berlin, Germany). Briefly, cells were lysed by the addition of 500  $\mu\text{l}$  lysis buffer G, followed by sonication ( $3 \times 10$  s, 30 W, VibraCell; Sonics and Materials Inc., Dunbury, USA). Then, 30  $\mu\text{l}$  of Invisorb50 carrier suspension was added to the lysate and it was incubated at room temperature for 5 min. Both carrier material and bound DNA were collected by centrifugation ( $6000 \times g$ , short spin), and the supernatant was preserved for subsequent determination of the protein content. DNA/carrier was washed thrice by resuspension in 1 ml wash buffer and brief centrifugation. Finally, DNA was eluted by the addition of 200  $\mu\text{l}$  pre-warmed elution buffer D and a 5-min incubation period at 60 °C. Finally, the carrier was removed by centrifugation (10 min,  $15,000 \times g$ ) and the DNA content of the supernatant was determined spectrophotometrically.

Protein concentration was determined using the micro-Lowry-based Protein Assay Kit (Sigma, Heidelberg, Germany), following the recommended protocol. Initially, proteins were precipitated from the preserved supernatants by the addition of 1/5 volume each of the desoxycholate and trichloroacetic acid solutions provided with the kit, and then they were redissolved in PBS, pH 7.4.

### 2.4. RNA isolation and quantitative RT-PCR

Isolation of RNA and RT-PCR were performed as described previously [19]. Briefly, total RNA was prepared using the RNeasy Mini Kit (Qiagen, Hilden, Germany) and 1  $\mu\text{g}$  was transcribed into cDNA by means of AMV reverse transcriptase (Promega, Mannheim, Germany). Quantitative PCR was performed in the iCycler (Bio-Rad, Munich, Germany). A 25  $\mu\text{l}$  reaction mixture consisted of 12.5  $\mu\text{l}$  HotStart Taq Master Mix (Qiagen), 1  $\mu\text{l}$  cDNA, and 0.5  $\mu\text{mol/l}$  of the specific primers for Erk2-US (5'-CATGCCGAAGCAC-CATTC AAG) and Erk2-DS (5'-GATAAGCCAAGACGGGCTGGAG). Initial denaturation at 95 °C for 15 min was followed by 40 cycles with denaturation at 95 °C for 30 s, annealing at 62 °C for 30 s, and elongation at 72 °C for 30 s. Quantities of  $\alpha$ -tubulin mRNA were used to normalize cDNA content.

## 2.5. Western blotting

Western blots were performed as previously described [20] using the following primary antibody for immunodetection: rabbit anti-phospho-p44/p42 MAP kinase (Thr202/Tyr204) polyclonal, purified Ig (PhosphoPlus p44/p42 Antibody Kit; New England Biolabs, Schwalbach, Germany). Loading control was performed using GAPDH.

## 2.6. Measurement of respiration

Oxygen uptake of the cells was measured at 30 °C in a thermostat-controlled chamber equipped with a Clark-type electrode (Paar Physica Oxygraph Respirometer; Bioenergetics and Biomedical Instruments, Innsbruck, Austria). For the calibration of the oxygen electrode, the oxygen content of air-saturated incubation medium was taken to be 217 nmol/ml O<sub>2</sub>. Oxygen-free conditions were adjusted by the addition of dithionite to the medium [21,22].

## 2.7. Electron microscopy

For electron microscopy, three independent cell preparations were used for each incubation strategy. After sedimentation at 320 × g at 4 °C, the cell pellet was fixed with a mixture of 4% formaldehyde and 0.4% glutaraldehyde for 1 h at 4 °C. Thereafter, the pellet was rinsed thoroughly with PBS (pH 7.4), postfixed in 1% osmium tetroxide for 1 h at 4 °C, dehydrated in a graded series of ethanol, en bloc contrasted with 1% uranyl acetate in 70% ethanol, and flat-embedded between two polyethylene foils in Durcupan (Fluka/Sigma, Deisenhofen, Germany). Each washing and incubation step was followed by sedimentation at 320 × g at 4 °C to collect the cells. Ultrathin sections (50–70 nm) were prepared with a Leica Ultracut UCT (Bensheim, Germany), mounted on Formvar-coated slot grids, and examined with a Zeiss transmission electron microscope 900 (Oberkochen, Germany).

## 2.8. Determination of cellular adenine nucleotide concentrations

Reverse-phase chromatography, as described in [21], was applied. For the determination, a 1-ml aliquot of cellular suspension was added to ice-cold perchloric acid (final concentration 1.04 M) and centrifuged at 20,000 × g for 1 min. The supernatant was neutralized by KOH/HEPES (2 M/0.3 M) and subjected to HPLC analysis with an L-6200 pump and an L-4250 UV/VIS detector (Merck-Hitachi, Darmstadt, Germany) at 254 nm using a 250 × 4 mm RP18 column packed with 5 μm Si particles. Adenine nucleotides were eluted with 0.2 M KH<sub>2</sub>PO<sub>4</sub>, pH 5.95, by a step gradient of methanol: 5 min, 0% CH<sub>3</sub>OH; 6 min, 4% CH<sub>3</sub>OH; 5 min, 12% CH<sub>3</sub>OH; and 1 min, 40% CH<sub>3</sub>OH; at a flow rate of 1.0 ml/min.

## 2.9. Determination of total intracellular thiols by flow cytometry

The intracellular thiol concentration was measured specifically by 5-chloromethyl-fluorescein diacetate (CMFDA) staining in flow cytometry, as described previously [23]. Briefly, cell samples were stained with CMFDA at a final concentration of 12.5 μM in phosphate-buffered saline for 15 min at room temperature. After washing, the cells were fixed in 1% paraformaldehyde and analyzed within 2 h by flow cytometry at λ<sub>EX</sub>=490 nm/λ<sub>EM</sub>=520 nm (FACSCalibur; Becton Dickinson, Heidelberg). Some experiments were performed using 5-(and-6)-((4-chloromethyl)benzoyl)amino)-tetramethylrhodamine (CMTMR) for thiol staining at a final concentration of 12.5 μM. Except for the flow cytometric analysis at λ<sub>EX</sub>=541 nm/λ<sub>EM</sub>=565 nm, the staining procedure was identical to that described for CMFDA. P19 cells were defined by forward/side scattering, and gated for analysis. The levels of intracellular thiols were indicated by mean fluorescence intensities [mfi] of stained probes versus negative controls.

## 2.10. Statistical analysis

All values are expressed as means ± standard deviation (S.D.) if not indicated otherwise. Differences between the groups were evaluated using an

unpaired Student's *t* test. A *P* value of <0.05 was considered to be statistically significant.

## 3. Results

### 3.1. Rapid pacing stimulates Erk-2 expression, induces cellular hypertrophy, and causes oxidative stress

In order to evaluate the relevance of the in vitro model of tachyarrhythmia described here, we determined the effect of rapid pacing on Erk-2 expression, the content of thiols, and the protein/DNA ratio in EBs. EBs were exposed to pacing at 2.0 Hz for 24 h. This treatment caused a significant increase in mRNA expression of Erk-2 in EBs compared to unpaced control bodies (351.6 ± 80.5% versus 100.0 ± 37.1%; *P* < 0.01, *n* = 4) (Fig. 1). Pacing with a frequency of 0.6 Hz, which is similar to the frequency of spontaneous contraction of EBs, did not stimulate Erk-2 mRNA expression (not shown). In order to provide additional evidence for the stimulation of Erk-2 expression, we used Western blot analysis to determine the amount of phospho-Erk1/2 that was dependent on the applied pacing frequency. In accordance with the altered Erk-2 mRNA levels, the quantity of phospho-ERK1/2 protein was found to be increased after 24 h of pacing at 2.0 Hz (136.5 ± 18.3 vs. 100 ± 17.3%; *P* < 0.05, *n* = 4; Fig. 2).

Hypertrophy of cardiomyocytes has been recognized as a further hallmark of cardiac tachyarrhythmia in vivo [5,20,24,25]. Therefore, we determined the protein/DNA ratio of EBs in order to document cellular hypertrophy that occurred as a consequence of rapid pacing. The corresponding data are presented in Fig. 3. After 24 h of pacing at 2.0 Hz, the protein/DNA ratio of the EBs was substantially increased (1.101 ± 0.04 vs. 1.000 ± 0.015 relative units; *P* < 0.05, *n* = 3; the unpaced control was set to 1.00). These data demonstrate that the in vitro model of cardiac tachyarrhythmia provides a good reflection of the cellular hypertrophy found in vivo after cardiac tachyarrhythmia.

In order to elucidate whether oxidative stress is induced in the in vitro model of cardiac tachyarrhythmia, as demonstrated in atrial fibrillation in vivo [8,9,26], EBs were subjected to rapid pacing and the content of cellular thiols was determined. Pacing at 2.0 Hz over 24 h caused a substantial decline of the intracellular content of free thiols by 24.9 ± 12.1% (0 Hz: 1490 ± 162 mfi; 2.0 Hz: 1128 ± 241 mfi; *P* < 0.05, *n* = 3), indicating substantial oxidative stress. In contrast, pacing at a rate of 0.6 Hz over the same period of time did not alter the thiol content (0.6 Hz: 1472 ± 60 mfi) (Fig. 4).

### 3.2. Rapid pacing impairs mitochondrial morphology and mitochondrial energy metabolism

To study the effect of rapid pacing on mitochondrial energy metabolism, we first studied mitochondrial morphology in the differentiated cardiomyocytes. The electron microscopic analysis revealed that rapid pacing caused significant changes in mitochondrial morphology. Unpaced controls were characterized by morphologically intact mitochondria exhibiting normal cristae structure. In contrast, rapidly paced cells contained

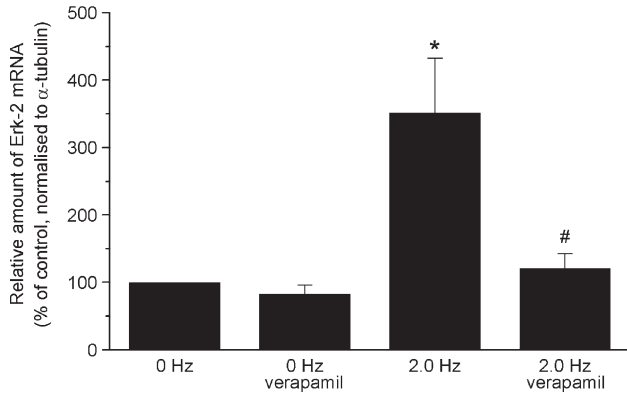


Fig. 1. Effect of rapid pacing on the mRNA expression of MAP kinase Erk2. Embryoid bodies derived from P19 cells were cultured in the presence or absence of 0.1  $\mu$ M verapamil and either subjected to electrical field simulation (at 2.0 Hz) or kept at spontaneous contraction rates (0 Hz) for 24 h. Quantitative RT-PCR was performed to analyze the effect of rapid pacing on the expression of Erk2 in in vitro differentiated cardiomyocytes. Amounts of Erk2 mRNA were significantly increased by 24 h pacing at 2.0 Hz. This increase was abolished by verapamil. \* $P$ <0.01 vs. unpaced control (0 Hz), # $P$ <0.05 vs. 2 Hz ( $n$ =4).

increased numbers of pale and swollen mitochondria, which partly showed cristaeolysis, as well as completely disrupted mitochondria. In addition, loss of plasma-membrane integrity was detected (Fig. 5).

In the next series of experiments, we determined endogenous oxygen consumption of the in vitro differentiated cardiomyocytes in culture medium. This experimental approach allows study of the effect of rapid pacing on the electron flux through complexes I–IV of the respiratory chain and essentially reflects the mitochondrial activity for ATP synthesis. Endogenous respiration was significantly lower in cells paced at 2.0 Hz compared to unpaced controls ( $60.4 \pm 6.4$  vs.  $236.6 \pm 5.4$  pmol  $O_2$ /min/mg protein,  $P$ <0.05,  $n$ =4) (Fig. 6). We did not find

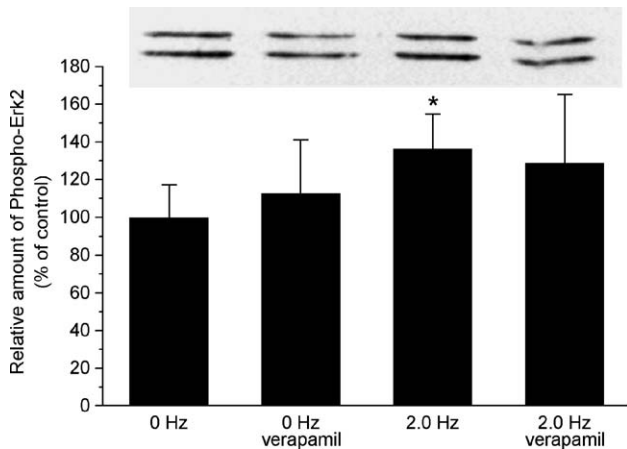


Fig. 2. Effect of rapid pacing on the activation of MAP kinase Erk1/2. Quantification of phospho-Erk2 protein content by densitometric analysis of Western blots of whole extracts from in vitro differentiated cardiomyocytes (10  $\mu$ g protein per lane). Western blots demonstrated an activation (phosphorylation) of MAP kinase ERK1/2 in response to pacing at 2.0 Hz (\* $P$ <0.05 vs. unpaced control (0 Hz);  $n$ =4). In the presence of 0.1  $\mu$ M verapamil, there was no significant change in the amount of phospho-ERK1/2.

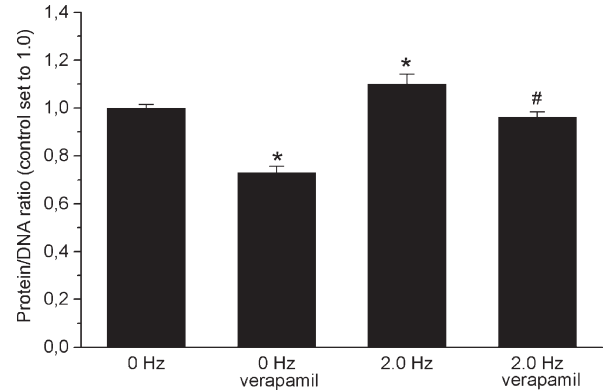


Fig. 3. Rapid pacing of in vitro differentiated cardiomyocytes causes cellular hypertrophy. Cellular hypertrophy was determined by measuring the protein/DNA ratio as described in Materials and methods. After 24 h of pacing at 2.0 Hz, there was a significant increase in the protein/DNA ratio when compared to pacing at 0.6 Hz. The presence of 0.1  $\mu$ M verapamil prevented the pacing-dependent hypertrophy and also resulted in a decrease of the protein/DNA ratio of unpaced cells. \* $P$ <0.05 vs. unpaced control (0 Hz); # $P$ <0.05 vs. 2.0 Hz ( $n$ =3).

significant changes in uncoupled respiration when we applied the uncoupler FCCP (carbonylcyanide-*p*-trifluoromethoxyphenyl-hydrazine), indicating no relevant impairment of the capacity of the respiratory chain. To elucidate whether the pacing-dependent decrease in endogenous respiration was caused by impairment of mitochondrial ATP synthesis or by impaired cellular ATP consumption, we compared the content of adenine nucleotides in differentiated cardiomyocytes of unpaced controls and cells exposed to 24 h of rapid pacing. In the case of impaired ATP synthesis, the cellular ATP levels should be decreased, and impairment of ATP consumption should result in an increased ATP content. Cellular adenine nucleotide concentrations in unpaced controls were  $88.15 \pm 4.9$  nmol/mg ATP,  $19.9 \pm 3.0$  nmol/mg ADP, and  $4.9 \pm 0.9$  nmol AMP ( $n$ =4). Twenty four hours of pacing at 2.0 Hz decreased ADP ( $-39.9 \pm 12.2\%$ ,  $P$ <0.05) and

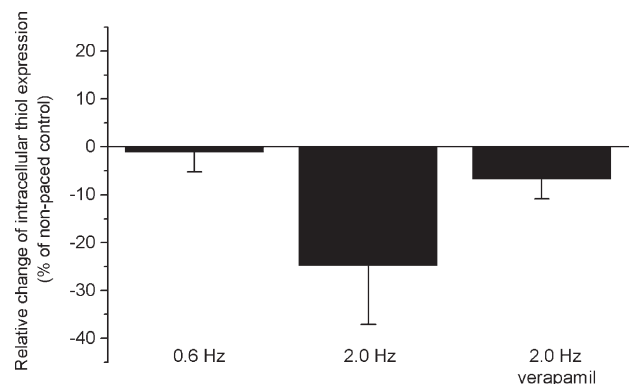


Fig. 4. Effect of rapid pacing on the content of cellular thiols as a marker of oxidative stress. Determination of intracellular thiol content in in vitro differentiated cardiomyocytes was performed by 5-chloromethyl-fluorescein diacetate (CMFDA) staining of intracellular thiols and flow cytometric analysis. Pacing at 2.0 Hz, but not at 0.6 Hz, decreased the intracellular thiol content compared to unpaced controls. Verapamil at a concentration of 0.1  $\mu$ M prevented the loss of free thiols (\* $P$ <0.05 vs. unpaced control (0 Hz), # $P$ <0.05 vs. 2.0 Hz,  $n$ =3).

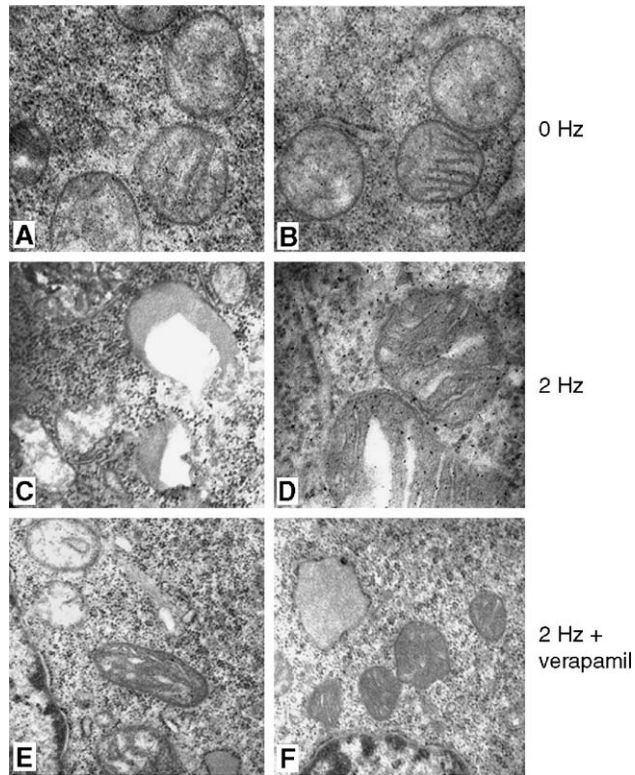


Fig. 5. Effect of rapid pacing on mitochondrial morphology. P19 cells were differentiated in vitro to embryoid bodies, which then were subjected to electrical stimulation at 0.6 and 2.0 Hz, and at 2.0 Hz in the presence of 0.1  $\mu$ M verapamil. (A, B) The electron microscopic appearance of mitochondria in untreated in vitro differentiated cardiomyocytes showed preserved morphology and well-defined cristae structures. (C, D) Pacing of cardiomyocytes at 2 Hz induced cell degeneration (pale, swollen mitochondria), partial cristaeolysis and destruction of cell membrane integrity. (E, F) Verapamil reduced mitochondrial degeneration, since fully intact mitochondria were observed. Magnification: 1:50,000.

ATP levels ( $-18.6 \pm 12.3\%$ ,  $P < 0.05$ ), but increased the AMP content by  $33.6 \pm 11.8\%$  ( $P < 0.05$ ) (Fig. 7). Thus, the lower rate of endogenous respiration measured after 24 h of pacing at 2.0 Hz in comparison with unpaced controls is almost certainly due to impaired mitochondrial ATP production.

### 3.3. Rapid pacing-induced modification of $Ca^{2+}$ influx causes increases in Erk-2 expression, oxidative stress and cellular hypertrophy, and mitochondrial alterations

To investigate the role of  $Ca^{2+}$  influx in the impairment of cardiomyocytes upon rapid pacing, we administered verapamil in order to diminish the  $Ca^{2+}$  influx by inhibiting  $Ca^{2+}$  channels of the L-type. We compared differentiated cardiomyocytes (EBs) that had been subjected to 24 h rapid pacing at 2 Hz in the presence and absence of 0.1  $\mu$ M verapamil. Verapamil attenuated the pacing-induced increase in Erk-2 mRNA by about two-thirds ( $351.6 \pm 80.5\%$  versus  $120.6 \pm 21.8\%$ ;  $P < 0.05$ ,  $n = 4$ ) and attenuated the increase of phospho-Erk1/2 protein (Figs. 3 and 4). Likewise, verapamil diminished the pacing-dependent decline in free thiols ( $-6.6 \pm 5.8\%$  with verapamil vs.  $-24.9 \pm 12.1\%$  without verapamil,  $P < 0.05$ ,  $n = 3$ ), indicating that oxidative stress occurring during rapid pacing is mediated

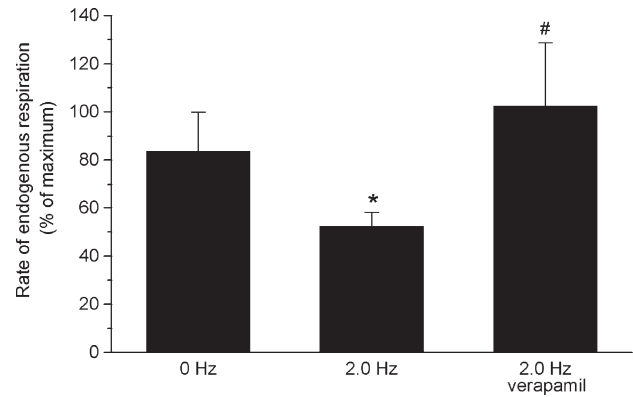


Fig. 6. Effect of rapid pacing on the rate of respiration of in vitro differentiated cardiomyocytes. Oxygen consumption of cardiomyocytes (about 12 mg cellular protein) incubated in growth medium was measured at 30 °C as described in Materials and methods. Mean  $\pm$  S.E.M. (%) of untreated controls ( $0.282 \pm 0.031$  nmol  $O_2$ /min/mg cellular protein), \* $P < 0.05$  vs. unpaced control (0 Hz), # $P < 0.05$  vs. 2.0 Hz;  $n = 4$ .

by  $Ca^{2+}$  influx (Fig. 4). Moreover, the presence of verapamil significantly reduced the increase in the protein/DNA ratio upon rapid pacing. This suggests that the spontaneously beating cardiomyocytes require a considerable  $Ca^{2+}$  influx via L-type calcium channels to respond to rapid pacing, with increases in protein synthesis and cell growth (Fig. 3).

Verapamil protects the mitochondrial morphology and mitochondrial function of cardiomyocytes exposed to rapid pacing to a significant extent (Figs. 5–7). The pacing-dependent drop in endogenous respiration and ATP levels, reflecting impaired oxidative phosphorylation in mitochondria, was attenuated by verapamil (endogenous respiration:  $117.0 \pm 3.0$  with versus  $60.4 \pm 6.4$  pmol  $O_2$ /min/mg protein without verapamil,  $P < 0.05$ ; change of cellular ATP:  $+2.2 \pm 13.5$  with versus  $-18.6 \pm 12.3\%$  of unpaced control without verapamil,  $P < 0.05$ ).

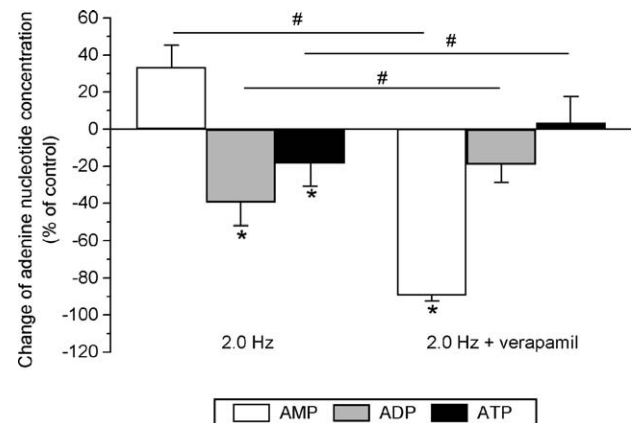


Fig. 7. Effect of pacing and verapamil on the adenine nucleotide pattern. Cardiomyocytes (about 12 mg cellular protein) were incubated in growth medium at 30 °C for 10 min. Samples of 1 ml were used for the determination of adenine nucleotide concentration as described in Materials and methods. The decrease in ATP and ADP as well as the increase in AMP in response to 2.0 Hz pacing reflects compromised mitochondrial ATP synthesis, which is ameliorated by 0.1  $\mu$ M verapamil. Mean  $\pm$  S.E.M. (%) of unpaced control, \* $P < 0.05$  vs. unpaced control (0 Hz), # $P < 0.05$  2.0 Hz vs. 2.0 Hz plus verapamil;  $n = 4$ .

## 4. Discussion

### 4.1. Stimulation of differentiated cardiomyocytes with an alternating electrical field as a model of cardiac tachyarrhythmia

In vitro pacing of isolated cardiomyocytes has been described by Ivester et al. [27] who showed that electrical field stimulation at a frequency between 0.125 and 0.5 Hz causes acceleration of protein synthesis in adult feline cardiomyocytes. In further studies from the same group, the cellular pacing model was used to induce sustained hypertrophic growth. Based on the results presented by Ivester et al. [27], we have established stimulation of in vitro differentiated cardiomyocytes with fast alternating electrical fields. These cardiomyocytes were derived from a P19 cell line. The molecular biology and electrophysiology of similar in vitro differentiated cells has been studied in detail [14,15,18,28]. In these cells, the expression pattern of ionic channels, including L-type  $\text{Ca}^{2+}$  channels, and contractile proteins is similar to adult terminally differentiated cardiomyocytes. Thereby, P19 cells represent a powerful model to study the regulation of myocardial differentiation processes [29]. P19-cell-derived cardiomyocytes form embryoid bodies (EBs) in culture. In this three-dimensional structure, various cells are electrically coupled. In addition to the presence of “atrial-like” and “ventricular-like” myocytes, which have been described according to the shape of the action potential, groups of cells have pacemaker activity. Therefore, whole EBs are beating spontaneously at a slow rate of about 0.5 Hz. In addition, EBs contain non-contractile, non-myocyte cells, which lead to non-homogeneous conduction as typically observed in myocardial tissue. Under the conditions applied in this study, electrical field stimulation induced synchronous contractions of EBs up to a rate of 180 bpm (3 Hz). To ensure 1:1 capture, we used a fixed pacing rate of 2.0 Hz. Similar to previous in vivo findings, we were able to demonstrate that pacing induced a hypertrophic response in vitro. In addition, 24 h pacing at 2.0 Hz induced upregulation of ERK2 mRNA and protein expression. Rapid pacing models have also shown that tachycardia induces ultrastructural changes and myolysis in vivo [1–5,30]. Similar to these in vivo models, we demonstrated significant ultrastructural and functional changes of mitochondria in our in vitro pacing model. Recent studies have demonstrated the importance of tachycardia-induced “oxidative stress” within atrial and ventricular myocardium [8,9,31]. Carnes et al. demonstrated the involvement of oxidative and nitrosive stress in “electrical remodeling” in a rapid atrial pacing model [8]; they demonstrated that 48 h of rapid pacing reduced tissue ascorbate levels and increased protein nitration. In an earlier study, the same group also showed increased rates of protein carbonylation in fibrillating human tissue [9]. These results provide evidence that tachycardias increase the concentration of reactive oxygen species (ROS) and reactive nitrogen species (RNS). The nitration and carbonylation of structural proteins impair myocardial energetic and electrophysiologic properties. Carnes et al. [8] proposed that oxidative stress mediates the alterations in atrial electrophysiologic parameters such as shortening of the atrial action potential. In

the ventricles, tachycardia-induced oxidative stress may be critical for the induction of apoptosis [31]. The occurrence of oxidative stress in our model was demonstrated by decreased levels of cellular thiols. These findings resemble the physiologic response described in vivo and, thus, contribute to the validation of our model.

### 4.2. Tachycardia-induced mitochondrial dysfunction

In the present study, to the best of our knowledge, we are the first to demonstrate in intact cardiomyocytes that 24 h of pacing at 2.0 Hz induces both impairment of mitochondrial ATP production structural mitochondrial changes. Reduced endogenous respiration, in combination with a decreased ATP/ADP ratio, clearly indicates reduction of mitochondrial ATP synthesis. Separate impairment of ATP utilization would lead to reduced respiratory chain activity accompanied by increased cellular ATP levels. Moreover, impairment of mitochondrial ATP synthesis is reflected by significantly increased AMP levels. Among mitochondrial enzymes, the most prominent candidate responsible for the impairment of mitochondrial ATP synthesis is the  $\text{F}_0\text{F}_1$ -ATPase. This has to be concluded from our finding that rapid pacing did not significantly affect uncoupled respiration which reflects the maximal capacity of mitochondrial oxygen consumption. Decrease in the activity of  $\text{F}_0\text{F}_1$ -ATPase has been reported in a canine model of pacing-induced cardiac failure [12]. However, the measurement of the  $\text{F}_0\text{F}_1$ -ATPase activity was not performed in intact cells, thus not allowing final conclusions concerning its pathophysiologic relevance. It is known that the maximal activity of many mitochondrial enzymes is expressed above the physiologic need. Therefore, small reductions in enzyme activity may be without any effect on ATP-synthesis in the intact cell. Energy failure may cause detrimental effects in the function of cardiomyocytes. Moreover, it has been shown that mitochondrial dysfunction, such as insufficient ATP synthesis or membrane permeabilization, can cause cell death due to apoptosis or necrosis [32,33].

### 4.3. $\text{Ca}^{2+}$ influx through L-type channels triggers changes in differentiated cardiomyocytes during rapid pacing

The increase in protein/DNA ratio and the activation of ERK1/2 was ameliorated by verapamil. This suggests that non-physiologic  $\text{Ca}^{2+}$  influx through L-type  $\text{Ca}^{2+}$  channels induced the increased protein synthesis (marker for cellular hypertrophy) in this model. In contrast, pacing at slow frequency did not increase either ERK1/2 phosphorylation or the protein/DNA ratio, demonstrating that the frequency of the alternating electrical field, but not the electrical field per se, triggers the development of hypertrophy. However, the fact that verapamil did not completely prevent the increase in ERK1/2 phosphorylation does not rule out the involvement of other signaling pathways in ERK activation.

It is known that an increase in the intracellular  $\text{Ca}^{2+}$  level activates cellular proteases and different hypertrophic pathways [25]. Recently, a  $\text{Ca}^{2+}$ -dependent signal transduction pathway leading directly to ERK activation has been suggested, involving

protein kinase A [34]. The final step of this pathway is the phosphorylation of ERK1/2, and, thereby, the expression of transcription factors (*c-jun*, *c-myc*, Elk1, ATF2, etc) is induced, which results in altered gene expression and enhanced protein synthesis. The impact of Ca<sup>2+</sup>-channel blocking drugs on myocardial hypertrophy has recently been investigated by Sanada et al. [35]; they showed that long-acting dihydropyridine Ca<sup>2+</sup>-channel blockers inhibit cardiac hypertrophy by inhibiting both a 70-kDa S6 kinase and ERK in vivo. Thus, the present study provides what we think is the first evidence that a tachycardia-altered Ca<sup>2+</sup> influx through L-type Ca<sup>2+</sup> channels initiates an ERK-dependent hypertrophic response.

Inhibition of cellular Ca<sup>2+</sup> entry by verapamil prevented the loss of intracellular thiols and attenuated mitochondrial changes. Thus, it seems that mitochondrial Ca<sup>2+</sup> plays a pivotal role in the impairment of mitochondria upon rapid pacing. Although no increase in mitochondrial Ca<sup>2+</sup> has been found during atrial fibrillation by electron probe microanalysis [36], inhibition of mitochondrial Ca<sup>2+</sup> influx by ruthenium red had a protective effect in a rat heart model of ventricular tachycardia [37]. Thus, we provide what we think is the first direct evidence that non-physiologic Ca<sup>2+</sup> entry is the primary trigger for mitochondrial dysfunction and oxidative stress within myocytes during tachycardia. The finding that verapamil protects from oxidative stress is supported by a recent study from Mason et al. [38]; they showed that mibefradil, which blocks L-type and T-type Ca<sup>2+</sup> channels, and verapamil prevent the oxidation of cellular constituents and have cytoprotective effects. Mibefradil was found to be more potent than verapamil at preventing lipid peroxide formation. However, due to significant side effects mibefradil is not used clinically, and, therefore, the demonstrated verapamil effect appears to be clinically more relevant. The concentration of verapamil used in this study (0.1 μM) is in the range of its reported IC<sub>50</sub> for ERG channels (143 nM) [39]. This concentration was chosen because at 10-fold higher concentrations viability and capturing of the EBs appears to be compromised. Similarly, beneficial clinical use of verapamil is based on a partial decrease of Ca<sup>2+</sup> influx, and it must under no circumstances fully block it. Since verapamil blocks ERG channels, it may alternatively affect cellular Ca<sup>2+</sup> homeostasis by attenuating the reaction potential. The possibility that changes in the reaction potential influence cellular Ca<sup>2+</sup> concentration has been demonstrated by Sah et al. [40].

ROS are also known to cause an increase in phosphorylation of ERK1/2 in cardiac myocytes and coronary arteries [41,42]. Pimental et al. [41] have shown that low- and high-amplitude stretch cause a ROS-dependent activation of ERK1/2. Interestingly, JNK was activated by high-amplitude stretch only. In the study of Pimental et al., activation of mitogen-activated protein kinases was associated with a differential induction of hypertrophic and apoptotic phenotypes. Thus, generation of ROS may have also contributed to the observed increase in ERK1/2 phosphorylation and cellular hypertrophy in our in vitro pacing model.

We have just started to investigate the molecular mechanisms that are altered during tachycardias. In the case of atrial arrhythmias, especially, knowledge regarding functional changes is limited because repetitive atrial biopsies are not feasible in

vivo. The model presented here, however, may help further in vitro experiments to address the functional role of different signaling pathways on tachycardia-induced myocardial alterations. This is particularly relevant as our findings indicate that cellular and molecular responses to rapid pacing in vitro largely mirror the pathophysiologic alterations observed in atrial tissue of patients with atrial fibrillation.

## Acknowledgements

We thank Katja Mook, Regine Widmayer, Karla Klingenberg, and Cornelia Müller for excellent technical assistance. This work was supported by grants from the “Kultusministerium des Landes Sachsen-Anhalt, Germany” (3517 A/0603M) and by the “Bundesministerium für Bildung und Forschung, Germany” (grant 01ZZ0407 and Kompetenznetz Vorhofflimmern, grant 01GI 0204).

## References

- [1] C.A. Morillo, G.J. Klein, D.L. Jones, C.M. Guiraudon, Chronic rapid atrial pacing: structural, functional, and electrophysiological characteristics of a new model of sustained atrial fibrillation, *Circulation* 91 (1995) 1588–1595.
- [2] A. Goette, C. Honeycutt, J.J. Langberg, Electrical remodeling in atrial fibrillation: time course and mechanisms, *Circulation* 94 (1996) 2968–2974.
- [3] S. Nattel, New ideas about atrial fibrillation 50 years on, *Nature* 415 (2002) 219–226.
- [4] J. Ausma, G.D. Dispersyn, H. Duimel, F. Thone, L. Ver Donck, M.A. Allesie, M. Borgers, Changes in ultrastructural calcium distribution in goat atria during atrial fibrillation, *J. Mol. Cell. Cardiol.* 32 (2000) 355–364.
- [5] J. Ausma, M. Wijffels, F. Thone, L. Wouters, M. Allesie, M. Borgers, Structural changes of atrial myocardium due to sustained atrial fibrillation in the goat, *Circulation* 96 (1997) 3157–3163.
- [6] A. Goette, M. Arndt, C. Röcken, T. Staack, R. Bechtloff, D. Reinhold, C. Huth, S. Ansorge, H.U. Klein, U. Lendeckel, Calpains and cytokines in fibrillating human atria, *Am. J. Physiol. Heart Circ. Physiol.* 283 (2002) H264–H272.
- [7] M. Arndt, U. Lendeckel, C. Röcken, K. Nepple, C. Zahn, C. Huth, S. Ansorge, H.U. Klein, A. Goette, Altered expression of ADAMs (a disintegrin and metalloproteinase) in fibrillating human atria, *Circulation* 105 (2002) 720–725.
- [8] C.A. Carnes, M.K. Chung, T. Nakayama, H. Nakayama, R.S. Baliga, S. Piao, A. Kanderian, S. Pavia, R.L. Hamlin, P.M. McCarthy, J.A. Bauer, D.R. Van Wagoner, Ascorbate attenuates atrial pacing-induced peroxynitrite formation and electrical remodeling and decreases the incidence of postoperative atrial fibrillation, *Circ. Res.* 89 (2001) e32–e38.
- [9] M.J. Mihm, F. Yu, C.A. Carnes, P.J. Reiser, P.M. McCarthy, D.R. Van Wagoner, J.A. Bauer, Impaired myofibrillar energetics and oxidative injury during human atrial fibrillation, *Circulation* 104 (2001) 174–180.
- [10] R.L. White, B.A. Wittenberg, Mitochondrial NAD(P)H, ADP, oxidative phosphorylation, and contraction in isolated heart cells, *Am. J. Physiol. Heart Circ. Physiol.* 279 (2000) H1849–H1857.
- [11] J. Ausma, W.A. Coumans, H. Duimel, G.J. Van der Vusse, M.A. Allesie, M. Borgers, Atrial high energy phosphate content and mitochondrial enzyme activity during chronic atrial fibrillation, *Cardiovasc. Res.* 47 (2000) 788–796.
- [12] J. Marin-Garcia, M.J. Goldenthal, G.W. Moe, Abnormal cardiac and skeletal muscle mitochondrial function in pacing-induced cardiac failure, *Cardiovasc. Res.* 52 (2001) 103–110.
- [13] M. Tsuboi, I. Hisatome, T. Morisaki, M. Tanaka, Y. Tomikura, S. Takeda, M. Shimoyama, A. Ohtahara, K. Ogino, O. Igawa, C. Shigemasa, S. Ohgi, E. Nanba, Mitochondrial DNA deletion associated with the reduction of adenine nucleotides in human atrium and atrial fibrillation, *Eur. J. Clin. Invest.* 31 (2001) 489–496.

- [14] M.W. McBurney, E.M.W. Jones-Villeneuve, M.K.S. Edwards, P.J. Anderson, Control of muscle and neuronal differentiation in a cultured embryonal carcinoma cell line, *Nature* 299 (1982) 165–167.
- [15] I. Skerjanc, H. Petropoulos, A.G. Ridgeway, S. Wilton, Myocyte enhancer factor 2C and Nkx-2.5 up-regulate each other's expression and initiate cardiomyogenesis in P19 cells, *J. Biol. Chem.* 273 (1998) 34904–34910.
- [16] A.M. Wobus, G. Wallukat, J. Hescheler, Pluripotent mouse embryonic stem cells are able to differentiate into cardiomyocytes expressing chronotropic responses to adrenergic and cholinergic agents and Ca<sup>2+</sup> channel blockers, *Differentiation* 48 (1991) 173–182.
- [17] V.A. Maltsev, J. Rohwedel, J. Hescheler, A. Wobus, Embryonic stem cells differentiate in vitro into cardiomyocytes representing sinusnodal, atrial and ventricular cell types, *Development* 44 (1993) 41–50.
- [18] Y.M. Zhang, C. Hartzell, M. Narlow, S.C. Dudley Jr., Stem cell-derived cardiomyocytes demonstrate arrhythmic potential, *Circulation* 106 (2002) 1294–1299.
- [19] A. Goette, T. Staack, M. Arndt, C. Röcken, C. Geller, C. Huth, S. Ansorge, H.U. Klein, U. Lendeckel, Increased expression of extracellular-signal regulated kinase and angiotensin-converting enzyme in human atria during atrial fibrillation, *J. Am. Coll. Cardiol.* 35 (2000) 1669–1677.
- [20] A. Bukowska, U. Lendeckel, D. Hirte, C. Wolke, F. Strigow, P. Röhnert, C. Huth, H.U. Klein, A. Goette, Activation of the calcineurin signaling pathway induces atrial hypertrophy during atrial fibrillation, *Cell. Mol. Life Sci.* 63 (2006) 333–342.
- [21] V. Stocchi, L. Cucchiari, M. Magnani, L. Chiarantini, P. Palma, G. Crescentini, Simultaneous extraction and reverse-phase high-performance liquid chromatographic determination of adenine and pyridine nucleotides in human red blood cells, *Anal. Biochem.* 146 (1984) 118–120.
- [22] B. Reynafarje, L.E. Costa, A.L. Lehninger, O<sub>2</sub> solubility in aqueous media determined by a kinetic method, *Anal. Biochem.* 145 (1985) 406–418.
- [23] M. Täger, A. Piecyk, T. Köhnlein, U. Thiel, S. Ansorge, T. Welte, Evidence of a defective thiol status of alveolar macrophages from COPD patients and smokers, *Free Radic. Biol. Med.* 29 (2000) 1160–1165.
- [24] J. Kajstura, X. Zhang, Y. Liu, E. Szoke, W. Cheng, G. Olivetti, T.H. Hintze, P. Anversa, The cellular basis of pacing-induced dilated cardiomyopathy. Myocyte cell loss and myocyte cellular reactive hypertrophy, *Circulation* 92 (1995) 2306–2317.
- [25] C. Ruwhof, A. van der Laarse, Mechanical stress-induced cardiac hypertrophy: mechanisms and signal transduction pathways, *Cardiovasc. Res.* 47 (2000) 23–37.
- [26] S.C. Dudley Jr., N.E. Hoch, L.A. McCann, C. Honeycutt, L. Diamandopoulos, T. Fukai, D.G. Harrison, S.I. Dikalov, J. Langberg, Atrial fibrillation increases production of superoxide by the left atrium and left atrial appendage: role of the NADPH and xanthine oxidases, *Circulation* 112 (2005) 1266–1273.
- [27] C.T. Ivester, R.L. Kent, H. Tagawa, H. Tsutsui, T. Imamura, G. Cooper, P.J. McDermott, Electrical stimulated contraction accelerates protein synthesis rates in adult feline cardiocytes, *Am. J. Physiol.* 265 (1993) H666–H674.
- [28] K.R. Boheler, J. Czyz, D. Tweedie, H.-T. Yang, S.V. Anisimov, A.M. Wobus, Differentiation of pluripotent stem cells into cardiomyocytes, *Circ. Res.* 91 (2002) 198–201.
- [29] M.A.G. Van der Heyden, M.J.A. van Kempen, Y. Tsuji, M.B. Rook, H.J. Jonsma, T. Opthof, P19 embryonal carcinoma cells: a suitable model system for cardiac electrophysiological differentiation at the molecular and functional level, *Cardiovasc. Res.* 58 (2003) 410–422.
- [30] F.G. Spinale, M. Tomita, J.L. Zellner, J.C. Cook, F.A. Crawford, M.R. Ziele, Collagen remodeling and changes in LV function during development and recovery from supraventricular tachycardia, *Am. J. Physiol.* 261 (1991) H308–H318.
- [31] D. Cesselli, I. Jakoniuk, L. Barlucchi, A.P. Beltrami, T.H. Hintze, B. Nadal-Ginard, J. Kajstura, A. Leri, P. Anversa, Oxidative stress-mediated cardiac cell death is a major determinant of ventricular dysfunction and failure in dog dilated cardiomyopathy, *Circ. Res.* 89 (2001) 279–286.
- [32] Y. Teshima, A. Akao, S.P. Jones, E. Marban, Carioride (HOE642), a selective Na<sup>+</sup>-H<sup>+</sup> exchange inhibitor, inhibits the mitochondrial death pathway, *Circulation* 108 (2003) 2275–2281.
- [33] M. Akao, B. O'Rourke, H. Kusuoka, M. Teshima, S.P. Jones, E. Morban, Differential actions of cardioprotective agents on the mitochondrial death pathway, *Circ. Res.* 92 (2003) 195–202.
- [34] T. Yamazaki, I. Komuro, Y. Zou, S. Kudoh, T. Mizuno, Y. Hiroi, I. Shiojima, H. Tokano, K. Kinugawa, O. Kohmoto, T. Takahashi, Y. Yazaki, Protein kinase A and protein kinase C synergistically activate the Raf-1 kinase/mitogen-activated protein kinase cascade in neonatal rat cardiomyocytes, *J. Mol. Cell. Cardiol.* 29 (1997) 2491–2501.
- [35] S. Sanada, K. Node, T. Minamino, S. Takashima, A. Ogai, H. Asanuma, H. Ogita, Y. Liao, M. Asakura, J. Kim, M. Hori, M. Kitakaze, Long-acting Ca<sup>2+</sup> blockers prevent myocardial remodeling induced by chronic NO inhibition in rats, *Hypertension* 41 (2003) 963–967.
- [36] J.G. Akar, T.H. Everett, R. Ho, J. Craft, D.E. Haines, A.P. Somlyo, A.V. Somylo, Intracellular chloride accumulation and subcellular elemental distribution during atrial fibrillation, *Circulation* 107 (2003) 1810–1815.
- [37] K. Kawahara, M. Takase, Y. Yamauchi, Ruthenium red-induced transition from ventricular fibrillation to tachycardia in isolated rat hearts: possible involvement of changes in mitochondrial calcium uptake, *Cardiovasc. Pathol.* 12 (2003) 311–321.
- [38] R.P. Mason, I.T. Mak, M.F. Walter, T.N. Tulenko, P.E. Mason, Antioxidant and cytoprotective activities of the calcium channel blocker mibefradil, *Biochem. Pharmacol.* 55 (1998) 1843–1852.
- [39] S. Zhang, Z. Zhou, Q. Gong, J.C. Makielski, T. Craig, Mechanism of block and identification of the verapamil binding domain to HERG potassium channels, *Circ. Res.* 84 (1999) 989–998.
- [40] R. Sah, R.J. Ramirez, R. Kaprielian, P.H. Backx, Alterations in action potential profile enhance excitation-contraction coupling in rat cardiac myocytes, *J. Physiol.* 533 (2001) 201–214.
- [41] D.R. Pimental, J.K. Amin, T. Miller, L. Xiao, J. Viereck, J. Oliver-Krasinski, R. Baliga, J. Wang, D.A. Siwik, K. Singh, P. Pagano, W.S. Colucci, D.B. Sawyer, Reactive oxygen species mediate amplitude-dependent hypertrophic and apoptotic responses to mechanical stretch in cardiac myocytes, *Circ. Res.* 89 (2001) 453–460.
- [42] R.A. Oeckler, P.M. Kaminski, M.S. Wolin, Stretch enhances contraction of bovine coronary arteries via an NADPH oxidase-mediated activation of the extracellular signal-regulated kinase mitogen-activated protein kinase cascade, *Circ. Res.* 92 (2003) 23–31.